Structure and stability of Ba–Cu–Ge type-I clathrates

2003 J. Phys.: Condens. Matter 15 5535

(http://iopscience.iop.org/0953-8984/15/32/313)

INSTITUTE OF PHYSICS PUBLISHING JOURNAL OF PHYSICS: CONDENSED MATTER

J. Phys.: Condens. Matter **15** (2003) 5535–5542 PII: S0953-8984(03)61981-8

Structure and stability of Ba–Cu–Ge type-I clathrates

Yang Li, Ji Chi, Weiping Gou, Sameer Khandekar and Joseph H Ross Jr

Department of Physics, Texas A&M University, College Station, TX 77843-4242, USA

E-mail: jhross@tamu.edu

Received 28 March 2003
Published 1 August 2003
Online at stacks.iop.org/JPhysCM/15/5535

Abstract

We have prepared samples of nominal type $Ba_8Cu_xGe_{46-x}$ by induction melting and solid state reaction. Analysis shows that these materials form type-I clathrates, with a copper content between $x = 4.9$ and 5.3, nearly independent of the starting composition. We used x-ray powder diffraction and single-crystal electron diffraction to confirm the cubic type-I clathrate structure, while electron microprobe measurements confirmed the stability of the $x \approx 5$ composition. This result differs from the corresponding Ag and Au clathrates and was not known previously due perhaps to the similar Cu and Ge form factors in x-ray diffraction. The observed composition adheres very tightly to a valence-counting scheme, in agreement with a Zintl-type stability mechanism. This implies a gap in the electronic density of states, also in contrast to the metallic behaviour of the Au and Ag analogues. Magnetization measurements showed a large diamagnetic response in the Ba–Cu–Ge clathrate. This behaviour is consistent with semiconducting or semimetallic behaviour and is similar to that of a number of intermetallic semiconductors.

1. Introduction

Silicon, germanium and tin form clathrate phases having framework structures in which the cages enclose single ions of the alkali metal, alkali earth, rare earth or halogen series [1–3]. Doping with metal atoms has led to a wide variety of electronic behaviours, including superconductivity in Ba_8Si_{46} [4] and in $Ba_8Ga_{16}Ge_{30}$ [5], ferromagnetism in $Ba_8Mn_2Ge_{44}$ [6] and a number of semiconducting compositions including the silicon-only material Si_{136} [7]. There has been considerable interest in these materials, for a number of potential applications including thermoelectric cooling [2, 3, 8]. There is the further potential for epitaxial growth in conventional semiconductor systems [9] and transition-metal and rare-earth-doped clathrates offer the possibility of new magnetic semiconductors.

We have studied the formation of Ba–Cu–Ge clathrates and report on the stable formation of clathrates with the type-I structure and compositions close to $Ba_8Cu_5Ge_{40}$. This composition forms preferentially for a range of starting compositions for ambient-pressure synthesis.

0953-8984/03/325535+08$30.00

The formation of Ba–Cu–Ge type-I clathrates has been reported previously [10]. It is known that Cu substitutes for Ge on framework sites, although the nearness of Cu and Ge in the periodic table makes identification of specific Cu atomic positions via x-ray analysis somewhat difficult.

In type-I germanium–barium clathrates, of nominal composition Ba_8Ge_{46}, germanium occupies three sites, which are Wyckhoff 6c, 16i and 24k sites in the cubic $Pm\bar{3}n$ (no 223) structure. This structure is the analogue of the $(Cl_2)_8(H_2O)_{46}$ gas clathrate [2]. Ba ions occupy 2a and 6d sites, corresponding to locations within the two distinct cages of the Ge framework. A stable Ba–Ge type-I clathrate of composition Ba_8Ge_{43}, with three framework vacancies per unit cell, has been prepared and found to be semiconducting [11]. The analogous Ba–Sn clathrate is predicted to be stable in the composition Ba_8Sn_{42} [12]. The latter can be understood in terms of the Zintl–Klemm concept [13], assuming that each Ba donates two electrons to the framework, satisfying the tetrahedral bonding requirements of the framework with four electrons per site, including vacancies. Semiconducting Ba_8Ge_{43} has one less vacancy per cell than is given by this argument, perhaps due to a slightly smaller electron transfer from Ba [11].

A number of transition metals have been incorporated into Ge and Si clathrates [10], predominantly by substitution at the 6c site. Au- and Ag-doped Ba–Si clathrates have recently been reported with a range of doping levels, exhibiting metallic and superconducting behaviour [14, 15]. Thus, these materials must lie outside the range of stabilization via bond filling of the Zintl type as seen in other clathrates. Au-doped Ba–Ge clathrate has also been reported to be metallic [11]. Hence, by analogy we expected the Cu-doped Ba–Ge clathrate to be a metal with a range of stable compositions, although the initial report described only $Ba_8Cu_6Ge_{40}$ [10]. However, our results show that Cu prefers to substitute in a relatively narrow range of composition, as detailed below. Furthermore, magnetic and transport measurements indicate this material to be semimetallic, in contrast to the Au analogue, and in the analysis and discussion section we show that a bond filling mechanism provides a good accounting for the stability of this phase.

2. Experiment

Ingots with nominal compositions $Ba_8Cu_xGe_{46-x}$, for $x = 2, 4$ and 6, were formed by rf induction melting and solid-state reaction. These samples will be referred to as Cu2, Cu4 and Cu6, respectively. Stoichiometric quantities of the elemental materials were finely powdered and pressed into BN crucibles, then induction heated in an argon atmosphere. The resulting ingots, exhibiting a metallic luster, were further reacted at 950 °C for 3 days, followed by 700 °C for 4 days, in evacuated ampoules. SEM and EDS analysis for the Cu2 and Cu6 samples showed these ingots to consist of large clathrate crystallites of typical size several-100 μm, with smaller crystallites of other phases. The outer portion of these ingots was physically separated and the central portion reserved for x-ray and magnetization measurements, giving a sample somewhat more concentrated in clathrate. Microprobe measurements were carried out on samples of the entire ingots.

Analysis by Cu Kα powder x-ray diffraction showed characteristic type-I clathrate reflections, with a few per cent diamond-structure Ge in the Cu2 and Cu4 samples. LeBail extraction and Rietveld refinement were performed using GSAS software [16, 17], giving lattice constants steadily decreasing with increasing nominal Cu concentration. The refinement process is rather insensitive to the difference between Cu and Ge, due to their nearness in the periodic table. Therefore, for better determination we used electron microprobe results, described below, to constrain the Cu/Ge ratio in the clathrate during the x-ray fitting process. Furthermore, in the fit we assumed the Cu to be located only on the 6c site, as reported for other transition-metal Ge clathrates. Figure 1 shows an x-ray fit thus obtained.

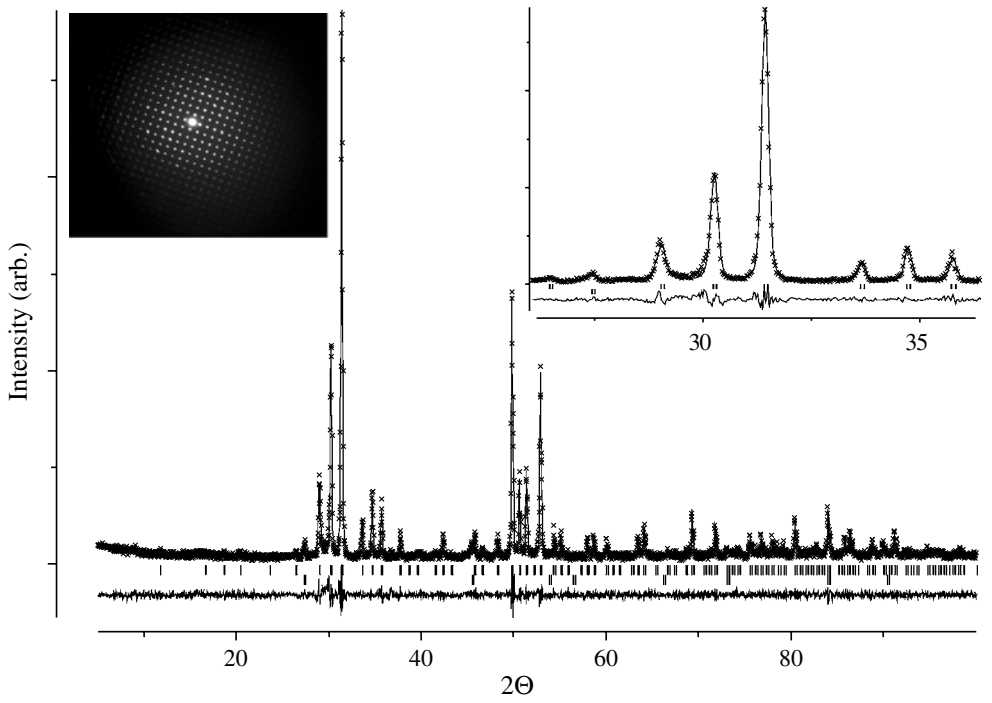

Figure 1. Cu Kα powder x-ray pattern for the Cu2 sample (nominal composition $Ba_8Cu_2Ge_{44}$), with fit and difference plot. The inset at the upper right is an expanded view. Vertical bars below the spectra indicate positions of the clathrate structure and Ge reflections. The inset at the left shows an electron diffraction pattern for the Cu6 sample, showing a cubic pattern characteristic of the type-I clathrate, with no superlattice structure.

X-ray analysis results are summarized in table 1, with the trend in some of the structural parameters also plotted in figure 2. We found that the Cu starting composition had a rather small effect on the resulting Cu and vacancy concentrations in the clathrate, with the Cu content very close to 5 per cell in all cases. The lattice constant exhibited a small decrease with increasing Cu content (figure 2). These results are consistent with those of [10]; values from that work are shown as filled squares in figure 2, placed at $x = 6$, which was the starting composition for that study. Bond lengths in figure 2 show some sample-to-sample variation. Error bars are smaller than this variation. We used isotropic thermal parameters for these fits and found the largest thermal parameter ($U_{iso} \approx 0.03$) for the Ba 6d site, occupying the larger cage, consistent with previous work on Ge clathrates.

The parameters x, y and z in table 1 are those for the $Pm\bar{3}n$ (no 223) structure; the 16i position is given by (x, x, x) and the 24k position, $(0, y, z)$. These parameters change very little with composition and the 6c site remains close to perfect tetrahedral symmetry (bond angles 109.5°). Figure 2 also shows the range of framework bond lengths, as the 6c–24k and 24k–24k bonds are the shortest and longest Ge–Ge bonds, respectively.

A powdered specimen from the Cu6 ingot placed on a grid for transmission electron microscopy showed the characteristic cubic diffraction pattern (inset of figure 1). Diffraction images from several crystallites in this sample were compared to simulations, giving a good match to the observations. A superlattice structure was previously identified in Ba_8Ge_{43}, attributed to preferential ordering of the framework vacancies in that material [11]. We saw

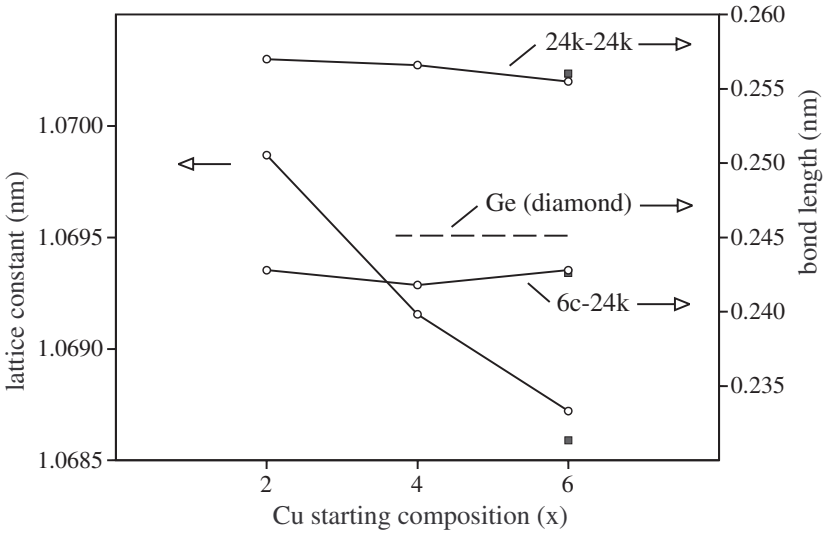

Figure 2. Lattice constant and representative framework bond lengths versus nominal Cu composition. Near-neighbour bond length for diamond-structure Ge is shown by the broken line. The shaded squares are from [10] for a sample of starting composition $x = 6$.

Table 1. Measured parameters for the three samples obtained from powder x-ray diffraction. The 6c angle is the larger 24k–6c–24k bond angle.

Sample	Cu2	Cu4	Cu6
a (nm)	1.069 87(1)	1.069 16(2)	1.068 72(1)
x	0.182 9	0.183 5	0.183 0
y	0.313 9	0.315 0	0.314 0
z	0.120 1	0.120 0	0.119 6
6c angle (deg)	110.2	109.8	109.9
Occupancy			
Ba 2a	1.00	1.00	0.93
Ba 6d	1.00	0.99	0.97
Ge 6c	0.09	0.10	0.10
Cu 6c	0.82	0.81	0.88
Ge 16i	1.00	0.99	0.97
Ge 24k	1.00	1.00	1.00
Ba/cell	8.0	8.0	7.7
Cu/cell	4.9	4.9	5.3
Ge/cell	40.6	40.5	40.1
Cu + Ge vacancy	0.49	0.59	0.61

no evidence of a superlattice pattern in our samples, indicating the Cu atoms and vacancies to be randomly distributed on the 6c and 16i sites.

Compositional analysis was carried out using a commercial wavelength dispersive spectroscopy (WDS) based electron microprobe apparatus and analysis system (Cameca). In these measurements the clathrate phase was identified in each sample, plus Ge, an oxide of approximate composition $BaGeO_2$ and Ge_3Cu_5 (Cu6 sample only). Although dispersed throughout the ingots, the latter two were below the x-ray detection limit. In the Cu4 sample

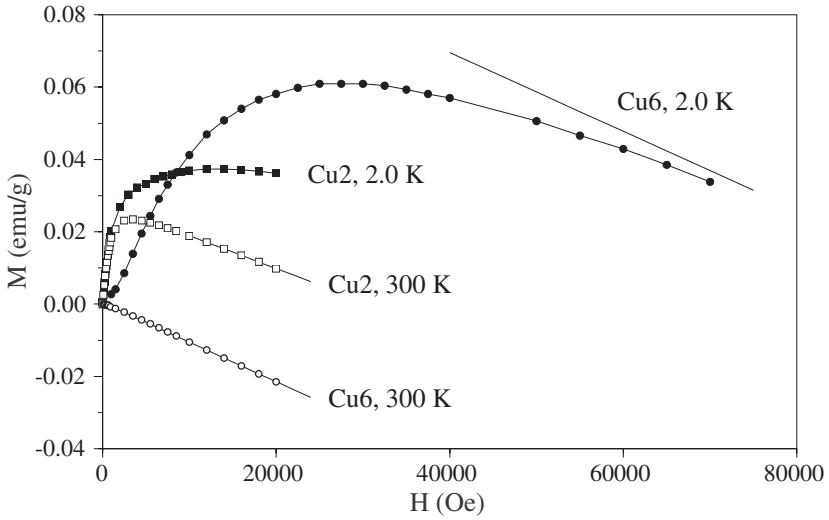

Figure 3. M versus H results for the Cu2 and Cu6 samples, at 2.0 and 300 K as labelled. Error bars are smaller than the symbols. Full curves through the 300 K data are least-squares fits, giving $\chi_{\rm dia} = -10.94(4) \times 10^{-7}$ emu g^{-1} (Cu6) and $-9.02(4) \times 10^{-7}$ emu g^{-1} (Cu2). The full curve above the Cu6, 2 K data has the same slope as the 300 K fit, showing slow saturation to this line. Curves connecting the 2.0 K data are guides to the eye.

a single localized Ge–Ba–S phase was detected, attributed to an impurity left after H_2SO_4 cleaning of the mortar and pestle. However, no S was detected in any of the other analyses. The Ba–Ge oxide was not found to contain Cu in any of the samples.

X-ray and WDS analysis both provide a relative measure of the number of atoms per cell, rather than an absolute composition. We produced the compositions in table 1 by assuming the largest site occupancy to be 100%. Scaling these results to lower values results quite quickly in vacancy concentrations which are unreasonable. For the Cu2 and Cu4 samples, this yields essentially 100% occupancy of the Ba sites, with framework vacancies appearing only on the 6c site. The Cu6-sample results are somewhat different, with vacancies appearing on the Ba 2a and framework 16i sites, as well as the framework 6c site. It appears that overloading the framework with Cu atoms forces vacancies to appear on the 16i site. The presence of Ba 2a vacancies is consistent with the behaviour observed in Ba_8Si_{46}. [18]

In the Cu2 and Cu4 samples, diamond-structure Ge appeared as inclusions within the abundant clathrate phase, indicating a phase separation during the solid state reaction process. For Cu6, an additional phase was observed, of nominal composition $GeCu_{1.65}$ or Ge_3Cu_5. (Diamond-Ge also contained about 1 at.% Cu.) Since the Cu content for Cu6 exceeded the clathrate stability limit, approximately 10% of the Cu appeared as Ge_3Cu_5 (or about 2 at.% of the entire sample), over and above the small change in Cu content of the clathrate. Ge_3Cu_5 has not been previously reported to our knowledge [19] and this structure may be stabilized by the adjacent phases. None of the reported Ge–Cu intermetallic structures ($GeCu_3$, $GeCu_5$ or Ge_2Cu_5) could be identified in the x-ray spectrum for the sample, nor could we identify reflections due to any other structures within our resolution.

Figure 3 shows M versus H results for the Cu2 and Cu6 samples, obtained using a commercial SQUID magnetometer (Quantum Design, Inc.). The Cu6 sample exhibited diamagnetism at high temperatures, which we fit to $\chi_{\rm dia} = -10.94(4) \times 10^{-7}$ emu g^{-1} (full curve in figure 3 for 300 K). At low temperatures the Cu6 sample also shows low-moment

ferromagnetism, which we attribute to a dilute concentration of random defects [20]. However, the high-field trend for the 2 K data is toward the same diamagnetic slope as at 300 K (upper curve in figure 3), though some moments are not completely saturated in the 70 kOe maximum field of our magnetometer. The Cu2 sample has a weak ferromagnetic phase visible at 300 K, but above saturation the slope was fitted to $\chi_{\rm dia} = -9.02(4) \times 10^{-7}$ emu g^{-1} (full curve), very similar to that of the other sample. Thus we identify the Cu–Ge clathrate to exhibit bulk diamagnetism with a susceptibility of approximately -10×10^{-7} emu g^{-1}.

3. Analysis and discussion

The hypothetical empty-cage clathrates Si_{46}, Ge_{46} and Sn_{46} are semiconducting as predicted by electronic structure calculations [12, 21, 22]. In filled Sn clathrates, the stable phase Cs_8Sn_{44} has two vacancies per cell, in accordance with the classic Zintl concept [13], in which the number of valence electrons on the framework is preserved to give the most favourable bonding configuration, and hence a filled band and semiconducting behaviour. Ternaries such as $Cs_8Ga_8Sn_{38}$ and $Cs_8Zn_4Sn_{42}$ can also clearly be treated this way [12].

The stable Ba–Ge phase Ba_8Ge_{43} [11, 23] can be treated as a Zintl phase with incomplete charge transfer from nominally divalent Ba. However, the ionic character of Ba is less clear than that of the alkali metals, as there is evidence for mixing of the Ba 5d orbitals into the conduction band [22, 24, 25]. On the other hand, for the Cu–Ge clathrate studied here, the valence counting argument works very well. If we assume Cu to have valence 1 and Ba valence 2, valence counting predicts the stable phase to be $Ba_8Cu_{(16/3)}Ge_{(46-16/3)} = Ba_8Cu_{5.3}Ge_{40.7}$. Or, if framework vacancies are allowed, one obtains compositions such as $Ba_8Cu_5Ge_{40.75}$. These values are quite close to those observed in our samples (table 1).

The formation of vacancies is not necessary by this argument. However, the presence of Cu causes the lattice parameter to contract relative to the Ba–Ge clathrate. Since Cu cannot occupy all of the 6c sites by valence counting, some Ge atoms must occupy this site, having a neighbour distance smaller than that of elemental Ge (figure 2). Framework vacancies may allow this strain to be accommodated more easily. With an increased Cu concentration, the valence count can also be maintained by inducing Ba vacancies, as observed in Cu6. This attests to the strong stabilizing influence of the valence count, in contrast to the situation in the analogous Ag and Au clathrates.

There are other intermetallics in which the valence count influences the stability, although the Zintl concept would not normally apply. These would include a large class of semi-Heusler alloys such as TiNiSn, an intermetallic semiconductor [26]. However, in that case the adherence to valence count is not nearly so strong as in a BaCuGe clathrate. What distinguishes the present case from other intermetallics is the fourfold-coordinated framework which enhances the stabilization of a local bonding configuration. This implies a rather ionic configuration for Cu, which would be more difficult to maintain for Au and which may explain the distinction between the Cu and Au clathrates.

The Zintl mechanism implies a deep minimum or gap in the electron density of states at the Fermi level, which is consistent with the large diamagnetic susceptibility that we have measured. This susceptibility is four times larger than observed for the Au clathrate [11] and larger than that of other group-IV clathrates of which we are aware. Per framework site, the susceptibility of the Cu6 sample is -95×10^{-6} emu mol^{-1}, comparable to that of the largest elemental diamagnets [27] and considerably larger than the value (-13×10^{-6} emu mol^{-1} or -1.4×10^{-7} emu g^{-1}) we obtain for the core susceptibility using standard parameters [28].

In tetrahedrally bonded elemental semiconductors, there is a near-cancellation of the paramagnetic and diamagnetic susceptibilities. A model for this behaviour [29] indicates that

the valence contribution to the diamagnetic susceptibility scales with $\langle r^2 \rangle$, as for molecular systems. However, the expansion of the clathrate framework relative to the zinc-blende lattice does not appear sufficient to explain the large magnitude of the diamagnetic susceptibility observed here. Furthermore, though there are structural similarities to graphite, we do not expect the clathrates to have the conjugated orbitals which give ring currents in aromatic molecules [28]. On the other hand, recent measurements [30] have shown a large diamagnetic response for the semimetal $RuAl_2$, as well as other intermetallic semiconductor systems such as the skutterudite $CoSb_3$. The mechanism for this is not known. However, it seems likely that the Cu clathrate is on the same footing with these systems and exhibits a narrow gap or pseudogap at the Fermi surface.

4. Conclusions

We have prepared type-I clathrates from different starting Ba–Cu–Ge compositions and find a preferred composition with the Cu content close to 5, rather than 6, per cell. Furthermore, the composition adheres rather tightly to a valence-counting scheme, which we attribute to the Zintl mechanism, in contrast to the Au and Ag analogues. This implies a semimetallic or semiconducting characteristic, contrasting with the reported metallic behaviour of the Au clathrate. A very large diamagnetic susceptibility was also observed, which matches the behaviour of other semiconducting and semimetallic intermetallics.

Acknowledgments

This work was supported by the Robert A Welch Foundation, grant no A-1526, and by Texas A&M University through the Telecommunications and Informatics Task Force.

References

[1] Ramachandran G K, Dong J J, Diefenbacher J, Gryko J, Marzke R F, Sankey O F and McMillan P F 1999 *J. Solid State Chem.* **145** 716
[2] Nolas G S, Weakley T J R, Cohn J L and Sharma R 2000 *Phys. Rev.* B **61** 3845
[3] Nolas G S, Chakoumakos B C, Mahieu B, Long G J and Weakley T J R 2000 *Chem. Mater.* **12** 1947
[4] Yamanaka S, Enishi E and Fukuoka H 2000 *Inorg. Chem.* **39** 56
[5] Bryan J D 1999 *Phys. Rev.* B **60** 3064
[6] Kawaguchi T, Tanigaki K and Yasukawa M 2000 *Appl. Phys. Lett.* **77** 3438
[7] Gryko J, McMillan P F and Marzke R F 2000 *Phys. Rev.* B **62** R7707
[8] Cohn J L, Nolas G S, Fessatidis V, Metcalf T H and Slack G A 1999 *Phys. Rev. Lett.* **82** 779
[9] Munetoh S, Moriguchi K, Kamei K, Shintani A and Motooka T 2001 *Phys. Rev. Lett.* **86** 4879
[10] Cordier G and Woll P 1991 *J. Less-Common Met.* **169** 291
[11] Herrmann R F W, Tanigaki K, Kawaguchi T, Kuroshima S and Zhou O 1999 *Phys. Rev.* B **60** 13245
[12] Myles C W, Dong J and Sankey O F 2001 *Phys. Rev.* B **64** 165202
[13] Kauzlarich S M (ed) 1996 *Chemistry, Structure, and Bonding of Zintl Phases and Ions* (New York: VCH)
[14] Herrmann R F W, Tanigaki K, Kuroshima S and Suematsu H 1998 *Chem. Phys. Lett.* **283** 29
[15] Nozue Y, Hosaka G, Enishi E and Yamanaka S 2000 *Mol. Cryst. Liq. Cryst.* **341** 509
[16] Larson A C and von Dreele R B 2000 *Technical Report* LAUR 86-748 Los Alamos National Laboratory
[17] Toby B H 2001 *J. Appl. Crystallogr.* **34** 210
[18] Kitano A, Moriguchi K, Yonemura M, Munetoh S, Shintani A, Fukuoka H, Yamanaka S, Nishibori E, Takata M and Sakata M 2001 *Phys. Rev.* B **64** 045206
[19] Villars P and Calvert L D 1991 *Pearson's Handbook of Crystallographic Data for Intermetallic Phases* (Metals Park, OH: ASM International)
[20] Li Y, Gou W, Chi J and Ross J H Jr 2003 *Preprint* cond-mat/0305369
[21] Zhao J, Buldum A, Lu J P and Fong C Y 1999 *Phys. Rev.* B **60** 14177

[22] Saito S and Oshiyama A 1995 *Phys. Rev.* B **51** 2628
[23] Carrillo-Cabrera W, Curda J, Peters K, Paschen S, Baenitz M, Grin Y and von Schnering H G 2000 *Z. Kristallogr.* **215** 321
[24] Moriguchi K, Munetoh S and Shintani A 2000 *Phys. Rev.* B **62** 7138
[25] Blake N P, Bryan D, Latturner S, Mollnitz L, Stucky G D and Metiu H 2001 *J. Chem. Phys.* **114** 10063
[26] Tobola J, Pierre J, Kaprzyk S, Skolozdra R V and Kouacou M A 1998 *J. Phys.: Condens. Matter* **10** 1013
[27] Gray D E (ed) 1972 *American Institute of Physics Handbook* 3rd edn (New York: McGraw-Hill) pp 5–224
[28] Mulay L N 1976 *Theory and Applications of Molecular Diamagnetism* ed L N Mulay and E A Boudreaux (New York: Wiley) p 289
[29] Hudgens S, Kastner M and Fritzsche H 1974 *Phys. Rev. Lett.* **33** 1552
[30] Mandrus D, Keppens V, Sales B C and Sarrao J L 1998 *Phys. Rev.* B **58** 3712